

고밀도 폴리에틸렌 / 에틸렌 - 프로필렌 랜덤 공중합체 블렌드

김 병 규 · 김 면 수 · 김 국 중* · 신 영 조 · 박 상 보
부산대학교 고분자공학과 · *대한유화(주) 연구개발실
(1989년 5월 27일 접수)

Blends of High Density Polyethylenes with Etylene-Propylene Random Copolymer

B. K. Kim, M. S. Kim, K. C. Kim,* Y. J. Shin, and S. B. Park
Dept. of Polymer Science & Engineering, Pusan National Uniersity, Pusan 609-735, Korea
** R & D Division, Daehan Petrochemical Co. Ltd., Ulsan 680-110, Korea*
(Received May 27, 1989)

요 약 : 평균분자량 및 분자량 분포가 다른 2종의 고밀도 폴리에틸렌과, 에틸렌 대 프로필렌의 중량 조성이 1대 1인 랜덤 공중합체 EPM을 twin screw extruder에서 용융블렌딩 하였다. EPM의 함량이 20 wt % 이하에서는 interlocked된 morphology를, 그리고 EPM의 함량이 이보다 증가할 수록 입자분산상의 morphology를 주사전자현미경으로 부터 관찰할 수 있었다. 아울러 EPM과 유사한 점도를 가진 폴리 에틸렌과의 블렌드가 유성학적 측면에서 보다 상용성이 우수함을 알 수 있었으며, 열 분석 결과 블렌드의 용점이 순수 폴리에틸렌의 용점 보다 다소 높게 나타났으며, 경도 및 굴곡탄성률은 각각 양, 및 음의 편차를 보였다.

Abstract : Two types of HDPE, with different MW and MWD, were melt mixed with an EPM in a twin screw extruder. SEM micrographs indicated interlocked morphologies at low EPM contents (<20 wt %), and particle-in-matrix structure was obtained as the EPM contents increase. Better rheological compatibility was obtained from blends with PE having similar viscosities to EPM, in general. Thermal analysis indicated a small increase in melting point for the blends. Small positive and negative deviations from the additive rule were noted from hardness and modulus measurements, respectively.

INTRODUCTION

The blends of semicrystalline polyolefins with ethylene-propylene copolymer(EPM) or with ethylene-propylene-diene terpolymer(EPDM), leading primarily to thermoplastic elastomer(TP

E), have widely been encountered in many laboratories and industries.¹⁻⁵ TPEs based on polyolefins are mostly composed of polypropylene(PP), up to approximately 15wt % of EP(D)M and high density polyethlene(HDPE), respectively. The rubbery component acts as an impact

modifier via multiple crazing and shear yielding during the process of fracture. With rubber inclusion, the tensile properties of PP matrix such as strength and modulus inevitably decrease. Following the literature,⁶ the addition of HDPE in PP/EP(D)M binary blends suppresses the decrease of tensile properties by forming partially crystalline HDPE domains in rubbery phase. To obtain a preferential dissolution of HDPE in rubbery domains, binary blend of HDPE with EP(D)M is often first prepared, followed by mixing with PP in the second stage.

When the literature concerning the binary blends of PE/PP, PE/EP(D)M, and PP/EP(D)M is reviewed, earlier works mostly devoted to PE/PP and PP/EP(D)M blends. On the contrary, PE/EP(D)M blends have received less attention in the literature,⁷ probably because of the minor technological need to toughen PE. However, fundamental structure-property relationships of these systems should be also of importance, especially in relation to the ternary blends based on these binary systems.

In this paper we consider the binary blends of PE with EPM. Two types of PE with different molecular weights (MW) and molecular weight distribution (MWD), leading to different viscosity functions, have been blended with EPM. Viscosity-composition curves, morphologies, thermal and mechanical properties of these blends have been experimentally determined. However, emphasis was put on the rheological characterizations of the blends.

EXPERIMENTAL

Two types of commercially available HDPE (Daehan Petrochemicals) and one type of EPM (Exxon) as received were used for blending. The two types of HDPE grade, designated PE-A and PE-B, differ from the other mainly in their MW and MWD (Table 1 and Fig. 1). The EPM used was a random copolymer containing 50 wt% ethylene. The blends of PE-A/EPM and PE-

Table 1. Molecular Characteristics of HDPE Components

Component	Grade	$10^{-3} \cdot \bar{M}_n$	$10^{-3} \cdot \bar{M}_w$	PDI
PE-A	Film	21.0	234.7	11.15
PE-B	Extension	21.3	182.5	8.59

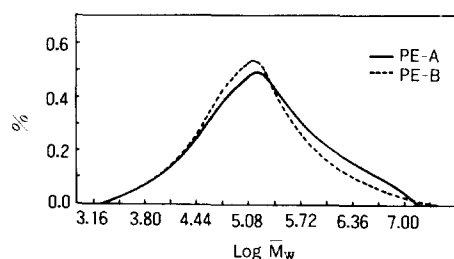


Fig. 1. Molecular weight distributions of HDPEs.

B/EPM were prepared from melt mixing in a twin screw extruder ($L/D=30$) at $210\sim 230$ °C, and 30 rpm. Rheological characterizations were made from a Rheometrics dynamic spectrometer (RDS 7700) in a cone-and-plate geometry, with cone angle of 0.1 rad and radius of 1.25cm. Measurements were carried out isothermally at 210 °C in nitrogen atmosphere. Frequency sweep was done at 15% strain level, and the level was determined from a strain sweep. Up to the level, samples showed linear viscoelastic behavior.

Morphologies of the blends were studied from scanning electron micrography (SEM), taken from the cryogenically fractured surfaces of injection molded tensile specimen, sputtered with gold before viewing. The melting peak temperatures (T_m) of the blends were measured from a differential scanning calorimetry (du Pont 990 DSC) at a heating rate of 10 °C/min.

Mechanical properties were determined from injection molded specimens following the ASTM procedures. Dumbbell specimens, punched out using a cutter, were elongated by using an Instron (4202) at a constant crosshead speed of 50 mm/min (ASTM D638). Flexural moduli were determined from three point bending test using the Instron (D790). All of the above mechanical

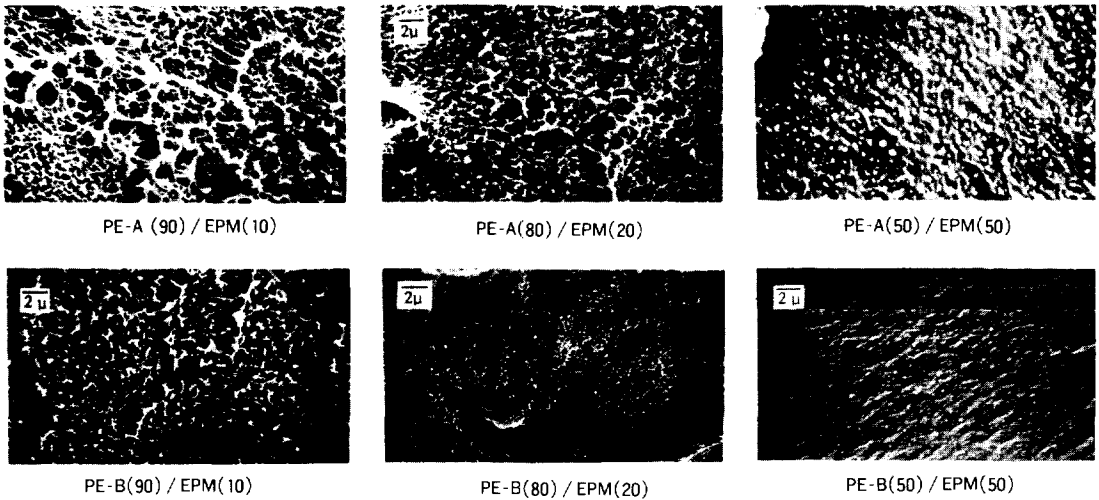


Fig. 2. Scanning electron micrographs of cryogenically fractured surfaces for PE-A / EPM and PE-B / EPM blends.

tests were done at room temperature. At least five runs were made and the results were averaged out to report.

RESULTS AND DISCUSSION

Morphology

SEM micrographs for PE-A / EPM and PE-B / EPM blends are shown in Fig. 2. In PE rich composition of the blends finely dispersed co-continuous morphologies are observed. However, as the EPM contents increase, particles-in-matrix morphologies dominate, i. e., the EPM particles are embedded in PE matrix.

Rheology

Complex viscosity functions for the components are shown in Fig. 3. Viscosities of PE-A are very close to those of EPM throughout the frequency range tested. Viscosities of PE-A, however, are slightly higher at low frequencies, and lower at high frequencies than those of EPM. This results in a viscosity function crossover at approximately $\omega = 2.0$ rad / s. The viscosities of EPM are higher than those of PE-B throughout.

The difference in viscosity functions between the PE-A and PE-B, especially at low frequency,

is the response of the different molecular parameters, viz. MW and MWD of the samples. Referring to Fig. 1, fair difference in MWD between the two samples is found in the high MW side of the distribution, an indication that the melt state properties are very sensitive to the fraction of long relaxation time.⁸

Viscosity functions, and viscosity vs. composition curves for the blends are shown in Figs. 4 ~7. At low frequency ($\omega = 10^{-1}$ rad / s), blends

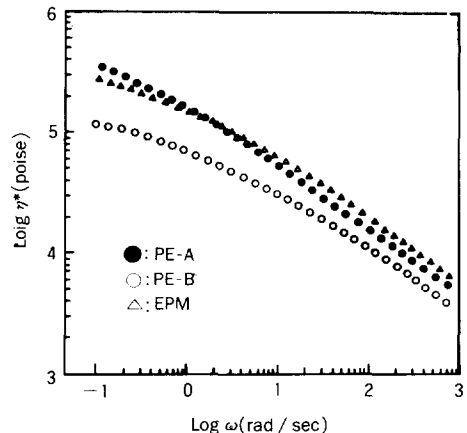


Fig. 3. Complex viscosity functions for the components.

of PE-A with EPM(Fig. 5) give negative deviation from the average of the two as regards to viscosities. Blends of PE-B with EPM(Fig. 7) also show the negative deviation near the midspan of the composition. However, a positive deviation is seen at PE content greater than 80 wt%. Notably, both of the binary blends follow the simple additive rule at high frequency.

Following Han,⁹ negative deviation of viscosity occurs when the droplets get sufficiently elongated, giving rise to threadlike fibrils that are aligned along the flow direction. If this is true for a certain blend system, the negative deviation

should become deeper with increasing frequency or rate of shear, and it was verified for several blend systems.⁹⁻¹² For the blends of PE-A with EPM, viscosities were measured both from RDS and capillary rheometers. The oscillatory flows between cone and plate correspond to almost simple shear flows, and the flows in capillary especially in the entrance region, more or less, correspond to elongational flows. Then, with more elongation in capillary flow than in RDS, we may expect greater negative deviation from capillary data. The results, however, do not confirm this, and in fact, they are reversed in tendency (Fig. 5.). One plausible explanation to this may be

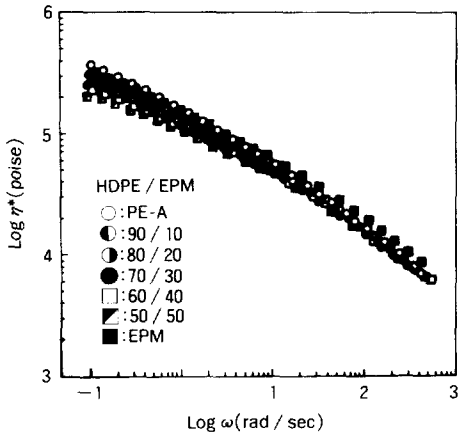


Fig. 4. Complex viscosity functions for PE-A / EPM blends.

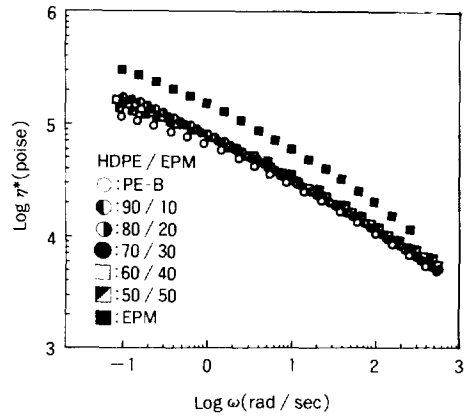


Fig. 6. Complex viscosity function for PE-B / EPM blends.

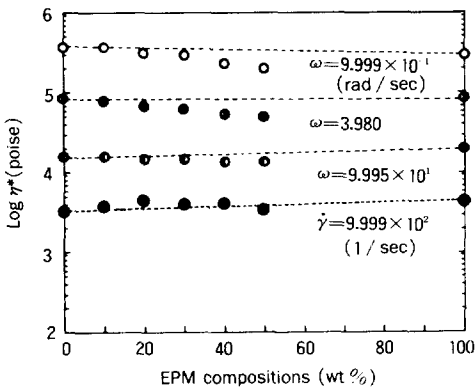


Fig. 5. Viscosity vs. composition for PE-A / EPM blends.

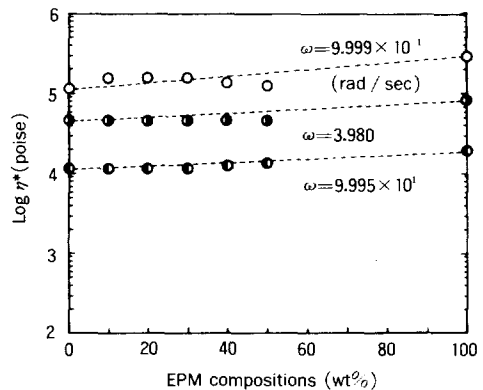


Fig. 7. Viscosity vs. composition for PE-B / EPM blends.

Blends of PE with EPM

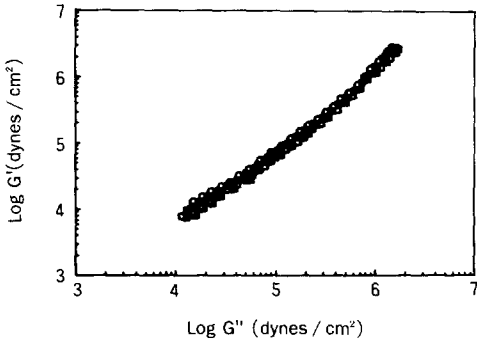


Fig. 8. G' vs. G'' for PE-A / EPM blends. Same symbols as in Fig. 4.

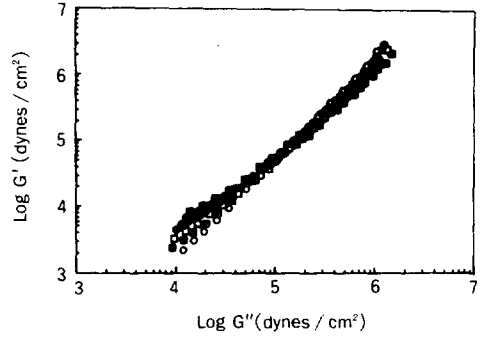


Fig. 9. G' vs. G'' for PE-B / EPM blends. Same symbols as in Fig. 6.

possible from the viscosity ratio of the components. The viscosity of EPM dispersed phase is greater than that of PE-A at high rate of shear. Therefore, the deformation of EPM particles do not follow those of continuous phase, prohibiting alignment of EPM phase along the flow direction. The negative deviation of viscosity from the simple additive rule, either in blend with PE-A or PE-B, should be the response of fine particle suspension of EPM in PE continuum. Such viscosity minimum at low shear has also been reported for many incompatible blends,¹²⁻¹⁷ and is generally regarded as a characteristic of fine particle suspension.

As mentioned earlier, at low EPM contents, PE-A / EPM as well as PE-B / EPM blends gave a finely dispersed and interlocked morphology. This probably is the reason why the viscosity-composition curves follow additive rule (PE-A / EPM), or show small positive deviation (PE-B / EPM).

Fig. 8 and 9 show G' vs. G'' plots for the blends. Such plots are virtually temperature independent, and give better comparison over the plots against frequency.¹⁸⁻²⁰

In the linear regions of the plots, the values of G' for the blends fall in between the two blend components. In PE-A / EPM blends, the values of G' monotonically is decreased with EPM inclusion. However, in PE-B / EPM blends, the variation of G' with EPM shows up and down,

and this should be related to the viscosity-composition curves given in Fig. 6. Another aspect considered in G' vs. G'' plot for blend is the width of G' values over the blend composition, with narrow width better rheological compatibility is generally indicated. It should be noted that the width of G' for PE-A / EPM blends is narrower than that of PE-B / EPM blends.

The crossover points ($G_c = G' = G''$) as a function of crossover frequency (ω_c) for the blends are given in Fig. 10. It has often been observed and reported²¹⁻²³ that the crossover modulus (G_c) is a measure of MWD, whereas the crossover frequency (ω_c) is a measure of MW. Mathematically the relations are given as $Y = AX^B$, where Y is G_c (or ω_c) and X is MWD (M_w / M_n) (or MW), and the adjustable parameters, A and B take negative values. The effective MW and MWD for PE-A / EPM blends monotonically decrease with EPM inclusion (Fig. 10a). On the contrary, the values of G_c and ω_c for the PE-B / EPM blends do not show monotonic changes with EPM. Particularly, the effective MW and MWD of the PE-B / EPM blends increase at 20 wt % EPM. With effective MW increases, the blend viscosity should also be increased. This is seen in Fig. 6.

Thermal Properties

Melting peak temperatures (T_m) determined from the DSC are shown in Fig. 11. In both of the binary blends, melting temperatures are sli-

ghtly higher for the blends than for the homopolymers, consistent with earlier findings by Greco et al.⁷ Who tested PE / EPM blends at

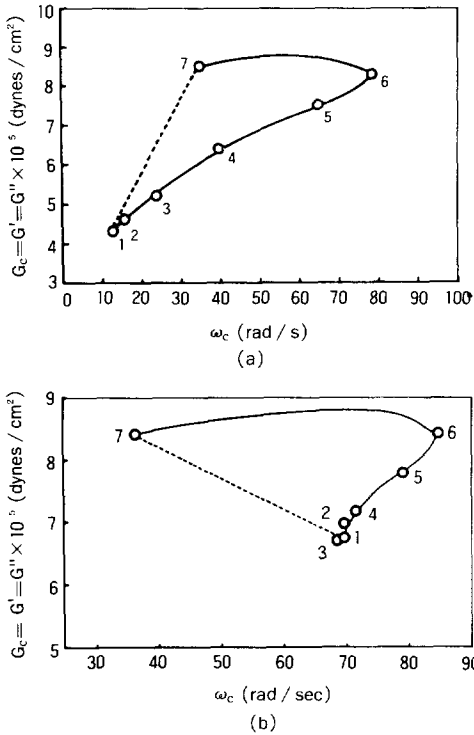


Fig. 10. Coordinates of $G_c = G' = G''$ crossover point : G_c vs. ω_c for PE-A / EPM(a) and PE-B / EPM (b) blends : PE-A / EPM=100 / 0(1): 90 / 10(2): 80 / 20(3): 70 / 30(4): 60 / 40(5): 50 / 50(6): 0 / 100(7): PE-B / EPM=100 / 0(1): 90 / 10(2): 80 / 20(3): 70 / 30(4): 60 / 40(5): 50 / 50(6): 0 / 100(7).

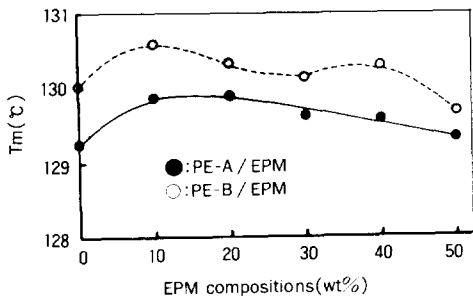


Fig. 11. Melting peak temperature(T_m) vs. composition for PE-A / EPM and PE-B / EPM blends.

a fixed composition(80 / 20) and with varying ethylene content of EPM. Probably, the EPM was able to dissolve the PE defective molecules, possibly low MW chains, leading to more perfect crystals or larger crystallites.⁷

Mechanical Properties

Rockwell hardness for the blends measured at room temperature is shown in Fig. 12. Hardness shows positive deviation in general, and does not make significant difference between the two types of PE. The flexural moduli for the blends indicate a negative deviation (Fig. 13), indication of incompatible nature of the blends.

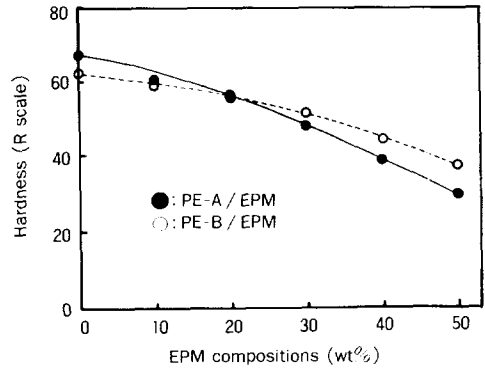


Fig. 12. Hardness vs. composition for PE-A / EPM and PE-B / EPM blends.

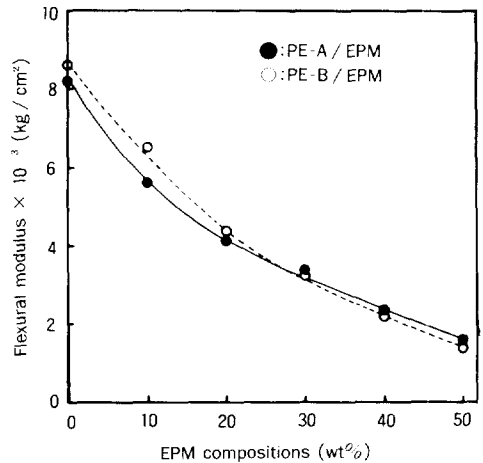


Fig. 13. Flexural modulus vs. composition for PE-A / EPM and PE-B / EPM blends.

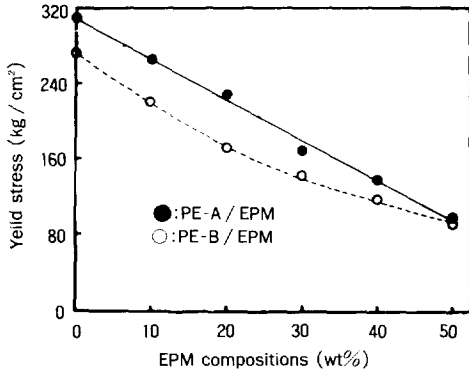


Fig. 14. Yield stress vs. composition for PE-A / EPM and PE-B / EPM blends.

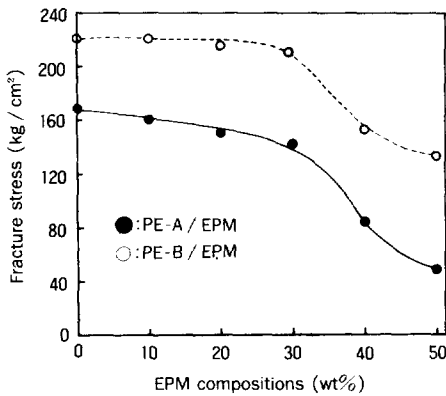


Fig. 15. Fracture stress vs. composition for PE-A / EPM and PE-B / EPM blends.

Yield stresses, measured from tensile tests, as a function of composition are given in Fig. 14. Yield stresses for PE-B / EPM blends show negative deviation with EPM content, however, those for PE-A / EPM blends drop linearly with EPM content. As a large strain response, the fracture stress for the blends (Fig. 15) shows a sharp drop on going from 30 to 40 wt% EPM in both types of blends. The change in morphological texture at this composition viz. from co-continuous structure to particle suspension, should be responsible for the sharp drop.

REFERENCES

1. J. Karger-Kocsis and I. Csikai, *Polym. Eng. Sci.*, **27**, 241(1987).
2. D. R. Paul and S. Newman ed., "Polymer Blends", Academic, New York, 1978.
3. N. R. Legge, G. Holden, and H. E. Schroeder ed., "Thermoplastic Elastomer", Hanser Publisher, New York, 1987.
4. P. Galli, S. Danesei, and T. Simonazzi, *Polym. Eng. Sci.*, **24**, 544(1984).
5. S. Onogi, T. Asada, and A. Tanaka, *J. Polym. Sci., A-2*, **7**, 171(1969).
6. J. Karger-Kocsis, A. Kallo, and V. N. Kuleznev, *Polymer*, **25**, 279(1984).
7. R. Greco, C. Mancarella, E. Martuscelli, G. Ratosta, and Y. Jinghus, *Polymer*, **28**, 1922 (1987).
8. J. E. Mark, A. Eisenberg, W. W. Graessley, L. Mandelkern, and J. L. Koenig, "Physical Properties of Polymers", Amer. Chem. Soc., Washington D. C., 1984.
9. C. D. Han, "Multiphase Flow in Polymer Processing", Academic, New York, 1981.
10. G. V. Vinogradov, B. V. Yarlykov, M. V. Tsebrenko, A. V. Yudin, and T. I. Ablazova, *Polymer*, **16**, 609(1975).
11. H. Van Oene, *J. Colloid Interface Sci.*, **40**, 448(1972).
12. S. J. Park, B. K. Kim, and H. M. Jeong, *Eur. Polym. J.*, in press.
13. L. Schmidt, *J. Appl. Polym. Sci.*, **23**, 2463 (1979).
14. K. J. Wang and L. J. Lee, *J. Appl. Polym. Sci.*, **33**, 431(1987).
15. L. A. Utracki, H. M. Catain, G. L. Bata, M. R. Kamal, and V. Tan, *J. Appl. Polym. Sci.*, **27**, 1913(1982).
16. C. D. Han, K. U. Kim, J. Parker, and C. R. Huang, *Appl. Polym. Symp.*, **20**, 191(1973).
17. B. K. Kim, H. M. Jeong, and Y. H. Lee, *J. Appl. Polym. Sci.*, in press.
18. C. D. Han and K. W. Lem, *Polym. Eng. Rev.*, **2**, 135(1982).

19. C. D. Han and H. H. Yang, *J. Appl. Polym. Sci.*, **33**, 1221(1987).
20. C. D. Han and H. H. Yang, *J. Appl. Polym. Sci.*, **33**, 1199(1987).
21. L. A. Utracki and B. Schlund, *Polym. Eng. Sci.*, **77** 367(1987).
22. M. M. Dumoulin, C. Farha, and L. A. Utracki, *Polym. Eng. Sci.*, **24** 1391(1984).
23. G. R. Zeichner and P. D. Patel, *Proc. 2nd World Cong. Chem. Eng.*, **6**, 333(1981).